Air-water Flow on a Stepped Chute downstream of a Piano Key Weir over Gravity Dams: An Experimental Study

Nismah Rizwan

Supervisors:
Prof. Dr. Jorge de Saldanha Gonçalves Matos
Dr. Maria Teresa Fontelas dos Santos Viseu

Instituto Superior Técnico, Universidade de Lisboa, Portugal
December 2019

Abstract

Gravity dams have been used for centuries as reservoirs for both, water and energy. To ensure that the structure has the desired output and cost-efficiency, the design of the crest, spillway, and stilling basin should be optimized. This dissertation combines the use of a Piano Key Weir and stepped spillway to analyze the skimming flow over it. All experiments were conducted, for a 4 cm step height, at an experimental facility built in LNEC in Lisbon, Portugal. Air entrainment and interfacial velocity were measured using a dual-tip phase intrusive probe developed at WRL, UNSW Australia. Data recorded by the probe was used to characterize the flow and its energy dissipation, by calculating parameters including: air concentration and velocity distributions, mean air concentration, representative flow depths, and specific energy. The cross-section was analyzed for four different discharges, and nine steps along the chute. The analysis revealed the occurrence of a skimming flow regime for all the tested discharges however, its initiation moved downstream with the increase in flow rate. The mean air concentration, as the water reached the bottom, decreased with increasing discharge, while the mean water velocity, flow depths, and specific energy increased. Additionally, the inlet and outlet keys of the PKW had a significant impact on the flow properties, particularly in the vicinity of the weir.

Key Words: Air Entrainment, Dual-tip Phase Intrusive Probe, Energy Dissipation, Piano Key Weir (PKW), Skimming Flow, Stepped Spillway.

1. Introduction

For years, dams have been used as both, reservoirs and outlets for energy, using water as the medium. The design of the crest and spillway has a significant impact on the output and cost-efficiency of the structure. An effective option is to combine the advantages of a Piano Key Weir (PKW) and stepped spillway. The unique structure of stepped spillways improves energy dissipation, while increasing air entrained in the flow. On the other hand, the labyrinth-type structure of the PKW results in an unconventional flow pattern over the crest, while increasing the discharge capacity, for the same width, by at least three times in

comparison with a Creager weir [1]. Conventionally, numerical models are used to simulate the flow over hydraulic structures however, the complexity of a PKW reduces the accuracy of this approach. Therefore, it is always more useful to test its geometry, along with the energy dissipation structure of the dam, on a physical model [2]. When using this approach, a factor of great interest is the equipment used to gather relevant data. A phase detection intrusive probe is one of the most common instruments used in the analysis of high velocity, air-water flows. In this context, the use of dual-tip probes is an interesting alternative, to the much-used single-tip probes, as it allows the collection of more information on flow properties.

This study presents a characterization of flow and energy dissipation over a stepped spillway fitted with a PKW, using a dual-tip phase detection intrusive probe developed at WRL, UNSW Australia [3]. The analysis was conducted on a test assembly set up at LNEC, in Portugal. This assembly has already been the focus of numerous studies [4] [5], which used a single-tip probe developed and calibrated by the USBR.

2. General Remarks

2.1. Piano Key Weir (PKW)

PKWs are a special type of labyrinth weirs, which were introduced by Lempérière and Ouamane, with the aim of providing a cost-effective way to increase the discharge capacity of already built dams [6]. They are often treated as safer alternatives to controlled spillways, such as gates since they encourage the free flow of water while fulfilling the same purpose [7]. As shown in Figure 1, the basic structure of a PKW is comprised of a narrow rectangular labyrinth with an inclined base on both, the upstream and downstream sides, commonly known as the inlet and outlet keys, respectively. A single unit of the PKW includes one complete inlet key with two half outlet keys on either side [2]. They are usually built with a small number of units, such that the crest width is not too large [7], yet water still flows through a longer length, increasing the overall discharge capacity at the same width of the spillway. The key dimensions of a PKW, illustrated in Figure 1, include: width, height, and slope of the inlet and outlet keys (w_i, w_o, P_i, P_o, S_i, S_o, respectively), thickness of the sidewalls (T_s), length of upstream (B_o) and downstream (B_i) overhangs, width of a single PKW unit (W_u), and overall width of the PKW (W). The effectiveness and stability of the structure depend primarily on the slope and 'crest length magnification ratio', which is a function of the balance between upstream and downstream overhangs [2]. Keeping this in view, four different types of PKWs exist today [2], of which Type A is the most common and has overhangs on both, the upstream and downstream sides.

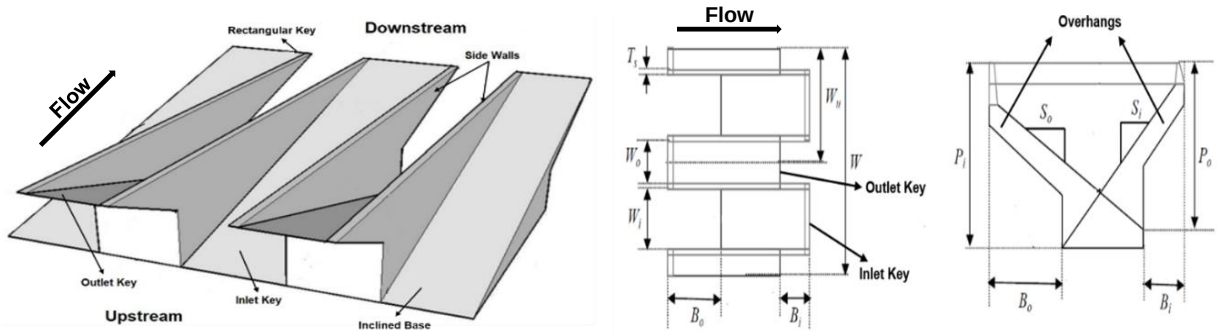

Figure 1: 3-D view of a typical PKW [8] (Left); Key dimensional parameters of a PKW [9]: Plan (Centre) & Side Views (Right)

2.2. Stepped Spillway

For centuries, stepped spillways have been used as a method of energy dissipation, based on the concept that when water moves through an inclined flow channel in a series of drops, it dissipates energy along the route, preventing the rapid increase in flow velocity and specific energy [10]. Flow over a stepped spillway is defined mainly by the unit discharge, step height, and spillway slope. Depending on these parameters, the flow may be characterized as nappe, transitional, or skimming flow, in order of evolution with an increase in discharge, at a constant spillway geometry [10]. This study analyzes the skimming flow regime, which is characterized by a coherent stream of water, while the spillway steps are fully submerged and do not interfere directly with surface flow [11]. Beneath the surface, the flow is typically in the form of vortices and occupies cavities formed by the steps. The bottom of flow, known as the 'pseudo-bottom', is formed by an imaginary line connecting the step edges [12]. When fitted with a PKW, flow over a stepped spillway changes slightly and may be divided into three distinct zones along the length, as described in Reis [4]. The initial flow is characterized by free jets from the inlet keys and a slowly evolving air-water skimming flow from the outlet keys. This is followed by a fully evolved three-dimensional skimming flow throughout the channel's cross-section, with a shift to two-dimensional flow in the final zone, near the bottom of the spillway.

2.3. Dual-tip Phase Intrusive Probe

High velocity air-water flows, with free surfaces, are often characterized by strong interactions between the particles of air and water. Flow analysis in such conditions may become quite complex, making conventional instrumentation, such as traditional Pitot tubes, unsuitable for high accuracy measurements [13]. In such cases, 'Phase Detection Intrusive Probes' provide a suitable alternative. These work on the principle of a conductivity probe, which makes measurements based on the rate at which air bubbles are pierced by the probe tip. The probe is usually connected with a data acquisition system, which transforms the detected information into voltage signals, defined by the different resistivities of the two media. The resulting signal is a function of the sampling duration, frequency, and threshold. Traditionally, conductivity probes have a single tip, however in recent years multiple designs have emerged with an additional 'trailing' tip, which allows the verification of data gathered by the main 'leading' tip and also the direct determination of interfacial velocity. For these probes, the tips should be as small as possible, and must be positioned adjacent to each other while being surrounded fully by water or air to detect the particles [3].

3. Experimental Facility

All the experiments in this study were conducted on an open flow channel installed at the National Laboratory of Civil Engineering (LNEC) in Portugal. The experimental facility is a fairly large scale model of a stepped spillway fitted with a PKW, shown in Figure 2, all made of 12 mm thick, clear, acrylic glass, which allows easy visualization of the flow. Water for the hydraulic circuit is withdrawn from an underground constant feed tank, and stored in an upstream reservoir, which can cater to discharges up to 200 L/s. From there, water flows over a PKW crest, 3.36 m from the ground, and into a 1 m wide rectangular open channel, lined with

a series of 4 cm high steps. The stepped channel has a slope of 1:0.75, viz. an angle of 53˚ from the horizontal. After flowing over the spillway, water enters a stilling basin, where it dissipates a portion of its remaining energy in the form of a hydraulic jump. Water exits this basin through a sluice gate, passes through a 0.8 m wide stabilization channel, and eventually flows back to the upstream reservoir. Hydrometers are located at key positions along the hydraulic circuit, to monitor the flow depth and estimate the discharge.

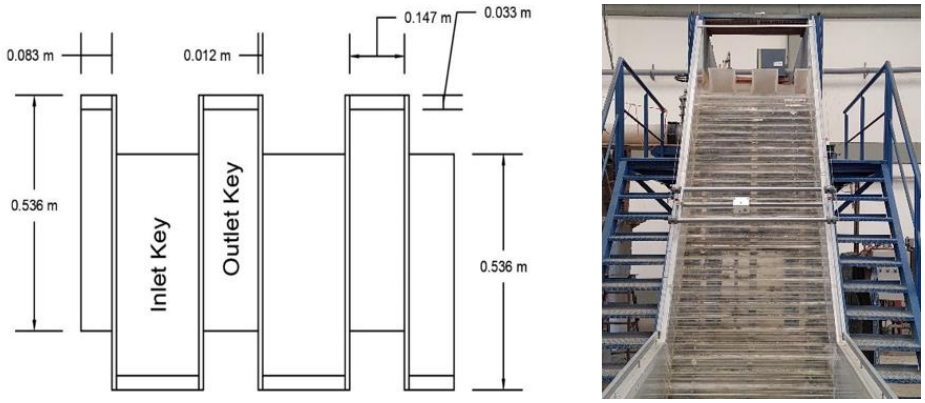

Figure 2: Key components of the experimental facility: Plan view of PKW with dimensions (Left); Stepped spillway (Right)

A dual-tip phase detection intrusive probe, developed at WRL, UNSW Australia, was used to gather data along the chute. The probe consists of two identical sensor tips, made of hypodermic needles, and called the 'Leading' and 'Trailing' tips. It has a set of conductivity sensors, which identify particles present in a solution by detecting their resistivity and converting it into electric signals. The probe has been reported to have a measurement accuracy of 4% for air concentration and 5-10% for interfacial flow velocity [3], and allows direct measurement of both. Post-processing of data, achieved with the help of a FORTRAN code [14], is required to determine other parameters. It makes use of the sampling frequency and time, the number of samples, and the threshold of air-water interface.

4. Experimental Methodology

Measurements were made for four different flow rates, which include: 60, 80, 140, and 180 L/s. For the three lower flow rates, measurements were made at 9 different steps, which include steps 15, 17, 19, 21, 24, 27, 30, 32, and 37. Whereas for a flow rate of 180 L/s, the same set was used with the exception of step 15, as it was out of range of the incoming jets of water. Flow was analyzed at six different location (verticals), each corresponding with key elements of the PKW, as depicted in Figure 3. Measurements were made at an additional four verticals (highlighted in Figure 3), amounting to a total of ten, to analyze the energy dissipation. This analysis was made only for steps 32 and 37, since they were the closest steps to the bottom of the spillway and the stilling basin, respectively, which the probe could reach. To record the desired data, the dual-tip probe was placed perpendicular to the pseudo-bottom, ensuring that the tips were in-line with the step and parallel to the flow direction. At each vertical, numerous measurements were made across the flow depth, by gradually raising the probe, up to a point where the void fractions at both tips reached 99%.

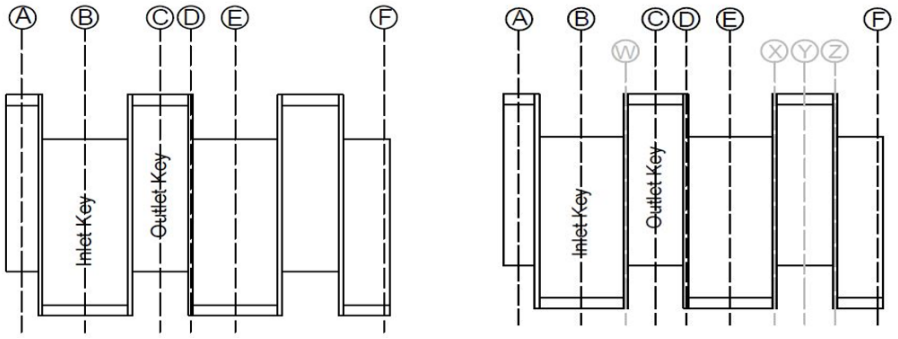

Figure 3: PKW with verticals highlighted for flow (Left) and specific energy (Right) analysis

While recording data, settings on the data acquisition software were kept constant for all the measurements. A sampling frequency of 20 kHz and a threshold of 80% [15] were used, while each measurement was made for a total of 45 seconds [13]. Once all the data was acquired, the air concentration (C) and interfacial velocity (v) profiles were examined, following which the characteristic depth (y_{90}), mean air concentration (C_{mean}), and equivalent clear-water depth (h_w) were calculated.

Normalized values of flow depth (y/y_{90}) and velocity (v/v_{90}) were also calculated, which were then fitted as a curve observing the Power law, which can accurately represent vertical velocity profiles while being applied to the entire flow region [16]. The relationship may be expressed as in Equation 1, where the exponent 'N', is a property of the channel bed and provides an indication of the resistance it imparts on the flow.

$$\frac{\boldsymbol{v}}{\boldsymbol{v_{90}}} = \left(\frac{\boldsymbol{y}}{\boldsymbol{y_{90}}}\right)^{1/N} \quad \textbf{(1)}$$

To study the energy dissipation, the head loss (ΔE) at the bottom of the chute was analyzed, which was determined as the difference between the maximum (E_{max}) and actual (E) specific energies at each step. As depicted in Equations 2 and 3, these components are both defined by Bernoulli's equation.

$$\boldsymbol{E_{max}} = \left(\boldsymbol{Z_{crest}} - \boldsymbol{Z_{step}}\right) + \boldsymbol{h_{PKW}} + \frac{\boldsymbol{U^2_{reservoir}}}{\boldsymbol{2g}} \quad \textbf{(2)}$$

$$\boldsymbol{E} = \boldsymbol{h_w}\cos\boldsymbol{\theta} + \boldsymbol{\alpha}\frac{\boldsymbol{U_w^2}}{\boldsymbol{2g}} \quad \textbf{(3)}$$

Where, Z_{crest} is the elevation of the spillway crest, Z_{step} is the elevation of the step edge, h_{PKW} is the height of water above the PKW in the upstream reservoir, $U_{reservoir}$ is the mean water velocity in the upstream reservoir, g is the acceleration due to gravity, Θ is the spillway slope, α is the kinetic energy coefficient, and U_w is the mean water velocity. In Equation 3, the equivalent clear-water depth was used to avoid the over estimation of specific energy that results from using the bulked flow depth [17]. The mean water velocity and kinetic energy coefficient were calculated using Equations 4 and 5 (adapted from [18]), respectively.

$$\boldsymbol{U_w} = \frac{\boldsymbol{Q}}{\boldsymbol{w} * \boldsymbol{h_w(avg)}} \quad \textbf{(4)}$$

$$\alpha = \frac{1}{U_w^2} * \frac{\int_0^1 \int_0^{y_{90}} (1 - C) v^3 \, dy \, dw}{\int_0^1 \int_0^{y_{90}} (1 - C) v \, dy \, dw} \quad (5)$$

Where, Q is the flow rate of water, w is the channel width, and h_w (avg) is the cross-sectional average equivalent clear-water depth at each step. During the analysis, results of the flow parameters were also compared with those of a previous study, by Gomes [5], which were obtained, using a single-tip probe, for the verticals C (outlet key) and E (inlet key), at steps 19 to 32, and for flow rates of 80 and 140 L/s.

5. Results and Discussion

5.1. Air Concentration Distribution

Generally, air concentration, at the analyzed verticals, was initially high, decreased slightly, and then increased continuously till it eventually became constant near the surface. The profiles typically varied across the channel's cross-section, depending on the vertical they correspond with, till a certain step, after which the profiles became relatively constant, indicating a shift from three-dimensional to two-dimensional flow. For all the tested discharges, the flow successfully entered the skimming flow regime however, the point of entry moved downstream with increasing flow rate. Once skimming flow was established, air concentration profiles, at each step, corresponding with similar keys depicted nearly identical trends. Close to the crest, air concentrations corresponding with the inlet keys were lower than the outlet keys however, this trend reversed as the flow moved downstream, suggesting the formation of cross waves within the flow. For all discharges, air concentrations at verticals A and F were the highest and lowest, respectively, across the cross-section, and indicated an influence of the channel's side walls.

The air concentration profiles obtained with the single and dual tip probes showed a fairly close comparison, for both the examined flow rates. Air concentrations recorded by the dual-tip probe were slightly lower for all the analyzed steps. After careful analysis, the reason for this was found to be an error in the adjustment of the voltage threshold while making measurements with the dual-tip probe. Occasionally, the threshold was set slightly higher than the chosen value, which could not be observed precisely due to the limited voltage scale of the data acquisition system. However, the difference in the results was generally low (within 10%), so repeating the measurements to gather a new set of data was deemed unnecessary.

5.2. Interfacial Velocity Profiles

Interfacial velocity profiles varied with the incoming discharge and distance from the crest, such that the velocity increased with both. In all cases, the velocity showed a rapid increase as the probe moved away from the pseudo-bottom but became constant closer to the surface. Velocity profiles corresponding with similar positions of the PKW were nearly identical at all steps and discharges. For the two smaller flow rates, velocities corresponding with the outlet keys were initially lower than the inlet keys but the profiles began to merge as the flow started becoming two-dimensional. For the higher discharges, velocities corresponding with the two types of keys were fairly intertwined and merged very close to the crest. This difference may be a result of the longer range of the water jets from the PKW as flow rate increased.

The normalized velocity profiles were also analyzed at each flow rate, and found to fit well as a function of the power law equation, except in a few cases, at the higher flow rates, before skimming flow was established. The exponent 'N' increased with an increase in the incoming discharge, while it decreased as the flow moved down the chute, reaching values close to 4, as expected [19], near the end of the spillway.

5.3. Characteristic Flow Depth

For all the tested flow rates, the maximum flow depth, and hence the characteristic flow depth, increased with an increase in discharge. This may be justified by the increase in the volume of water flowing over the chute. At all discharges, the characteristic depth was initially high, varied along the channel as a series of weak waves, with short-lasting fluctuations, until it eventually became constant near the base of the chute. This pattern is in accordance with the skimming flow regime.

5.4. Mean Air Concentration

The graphs in Figure 4 show that mean air concentrations obtained from the dual-tip probe were lower than the ones from the single-tip probe for all the analyzed steps. This may again be attributed to the imprecise allocation of the voltage threshold during experimentation. The difference between the two probes remained relatively constant, while the trend of variation of each was similar for the two keys, across the chute's length.

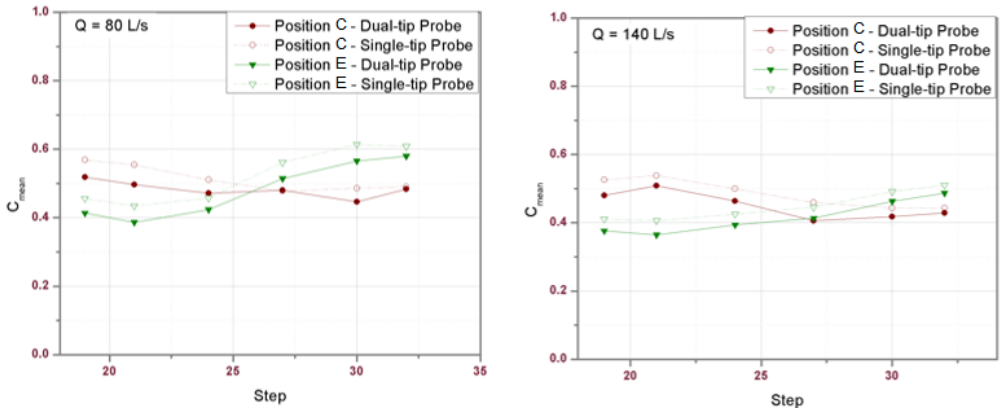

Figure 4: Mean air concentrations obtained with the dual-tip and single-tip [5] probes at 80 (Left), and 140 L/s (Right)

As seen in Figure 5, the mean air concentration, measured with the dual-tip probe, varied within a small range of values, which widened as the incoming flow rate increased. At all discharges, the mean air concentrations corresponding with the outlet keys were higher than the inlet keys, which occurred up to a certain step after which the trend reversed. The overall average value of the mean air concentrations decreased slightly as the flow rate increased.

5.5. Equivalent Clear-water Depth

The graphs in Figure 6 show that the difference between the two probes was more pronounced in the depths corresponding with the inlet key, i.e. the vertical E, which may be due to the slightly bigger gap in values of mean air concentration, as observed in Figure 4, because the clear-water depth depends significantly on it.

The graphs also show that the equivalent clear-water depth corresponding with the outlet key tends to increase over the channel's length, while the opposite can be seen for the inlet key.

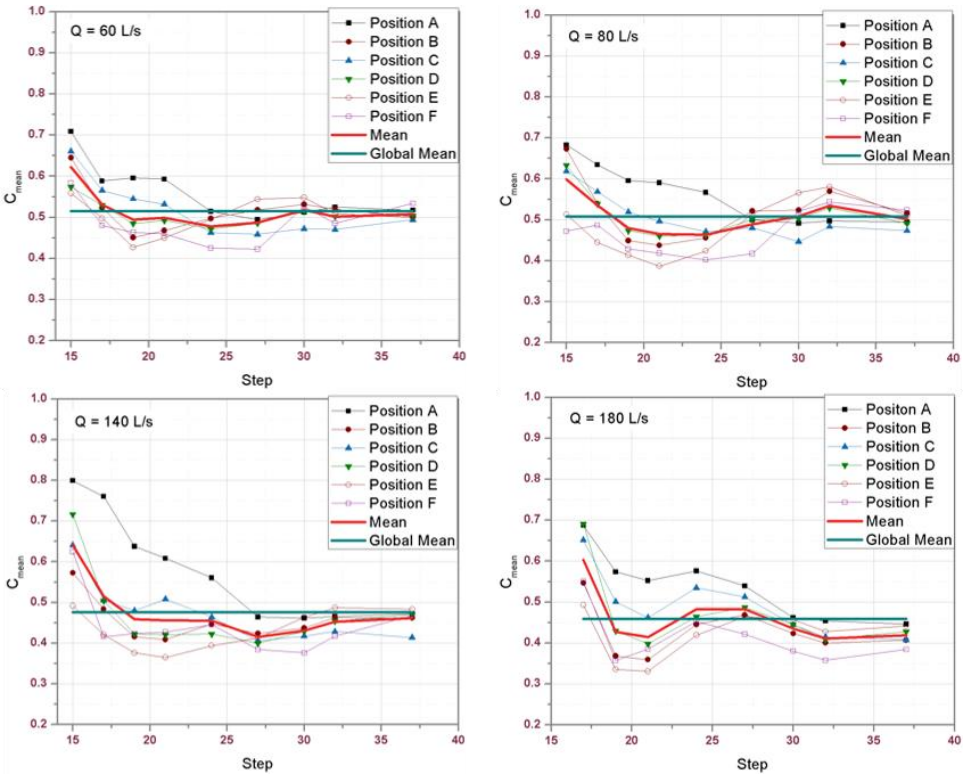

Figure 5: Mean air concentrations at 60 (Top left), 80 (Top right), 140 (Bottom left), and 180 L/s (Bottom right)

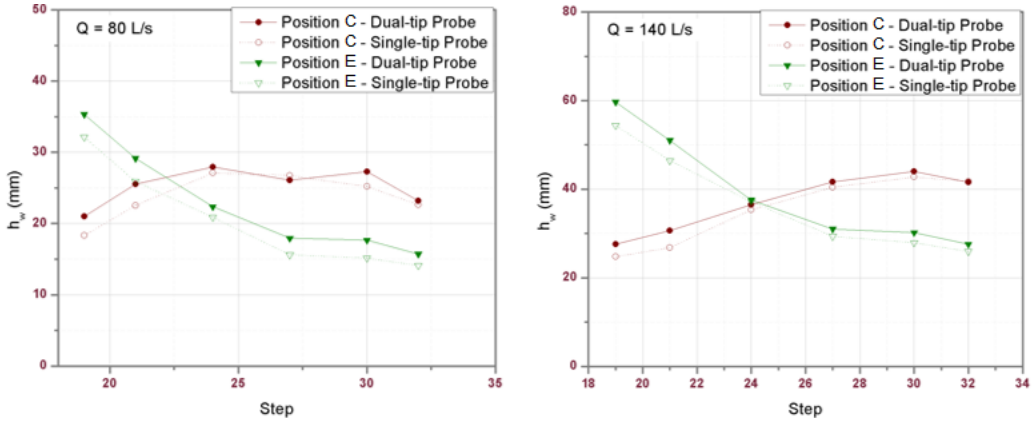

Figure 6: Equivalent clear-water depths obtained with the dual-tip and single-tip [5] probes at 80 (Left), and 140 L/s (Right)

As measured with the dual-tip probe, the equivalent clear-water depth increased with an increase in the flow rate, as shown in Figure 7. Typically, depths corresponding with the inlet keys were initially high but decreased as the flow moved downstream and eventually became constant near the bottom, whereas depths corresponding with the outlet keys exhibited the opposite trend. Since the equivalent clear-water depth represents the flow depth that would be achieved without air, it was always found to be lower than the characteristic depth.

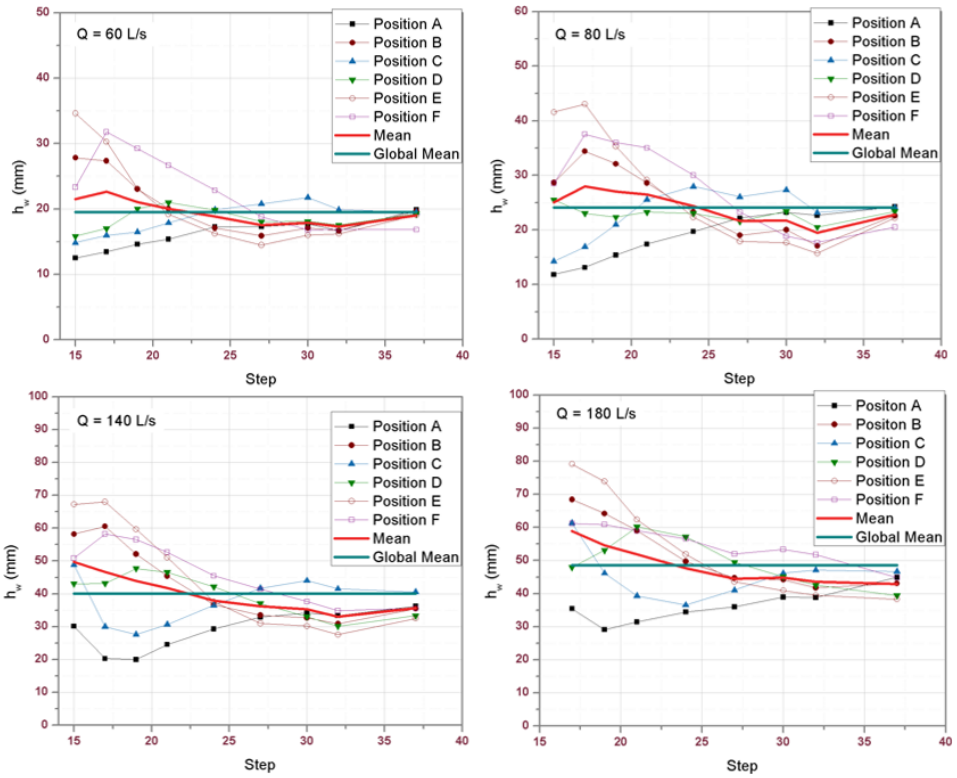

Figure 7: Equivalent clear-water depths at 60 (Top left), 80 (Top right), 140 (Bottom left), and 180 L/s (Bottom right)

5.6. Energy Dissipation of the Flow

All parameters involved in the analysis of energy dissipation across the stepped chute are presented in Table 1. Prior to making the desired computations, the mean air concentrations and flow depths were analyzed at steps 32 and 37, to study the cross-sectional uniformity of flow. The variation of these along the cross-section, and from one step to the other, was fairly low, which may be taken as an indicator that uniform flow may be achieved soon after step 37. At each step, the characteristic and equivalent clear-water depths increased with an increase in discharge, while the mean air concentrations decreased.

Table 1: Parameters involved in energy analysis at steps 32 and 37 for Q = 60, 80, 140, and 180 L/s

Parameter	Q = 60 L/s		Q = 80 L/s		Q = 140 L/s		Q = 180 L/s	
	Step 32	Step 37	Step 32	Step 37	Step 32	Step 37	Step 32	Step 37
C_{mean}	0.560	0.562	0.540	0.540	0.479	0.509	0.466	0.456
h_w (mm)	14.781	15.008	19.633	18.990	30.928	29.243	38.772	37.084
N	4.214	3.790	4.462	4.088	4.285	4.071	4.588	4.091
U_w (m/s)	4.059	3.998	4.075	4.213	4.527	4.787	4.643	4.854
α	1.061	1.187	1.154	1.188	1.109	1.134	1.166	1.210
E (m)	0.900	0.976	0.989	1.086	1.177	1.343	1.304	1.476
$\Delta E/E_{max}$	0.560	0.601	0.520	0.559	0.441	0.464	0.391	0.419

The velocity profiles obtained here were also checked for their adaptability to the Power law curve, to determine the exponent 'N', since this parameter is an indicator of the channel bed's resistance to flow and has a significant impact on the specific energy. The obtained values were close to 4, which is as expected for flows close to the bottom of the spillway. The mean water velocity increased with an increase in flow rate. The values of 'α' were between 1.1 and 1.2 for all the analyzed discharges, which is in accordance with previous similar studies [18]. The values in Table 1 clearly indicate that lesser energy was lost from the flow at higher discharges, while the relative head loss was greater as the distance from the crest increased.

6. Conclusions

As intended, the tested structural design was quite successful in breaking the force of water at all flow rates, particularly the higher ones, while encouraging air entrainment in the flow. Measurements made with the dual-tip probe were fairly comparable with the single-tip probe at 80 and 140 L/s. Keeping this in view, use of the dual-tip probe may be preferred as it provides more information on the flow characteristics, such as the direct measurement of interfacial velocity, while gathering two separate sets of data at each point.

The use of a PKW as the spillway's crest had a significant impact on the flow characteristics. The flow over the inlet keys was quite smooth and entered the spillway as a steady stream, while the flow over the outlet keys was more restricted and entered the chute as a jet. This difference resulted in the formation of cross-waves, which was often observed in the flow profiles at various locations along the cross-section. The side walls of the flow channel also had a considerable impact on the entrainment of air at all discharges however, this influence was significant only till a certain distance from the crest.

At all the tested discharges, the flow exhibited skimming flow, which was achieved beyond the influence of the PKW's jets. The overall flow depth increased with discharge, while the air entrainment was greater near the surface. In general, the characteristic and equivalent clear-water depths were higher near the crest, and tended to decrease as the water moved downstream. Additionally, the interfacial velocity was found to increase with discharge and distance from the crest, while the profiles were mostly found to fit well as a Power law curve, with the values of 'N' being within the expected range for skimming flows in open channels.

Analysis of the flow properties at steps 32 and 37 indicated that cross-sectional uniformity of flow was not achieved at any of the tested discharges. However, the flow moved quite close to it by step 37. As anticipated, the head loss, relative to the maximum energy, increased as the flow moved from the crest to the bottom. The relative roughness of the surface exposed to the flow decreased as the discharge increased, due to higher equivalent clear-water depths. As a result the head loss was lower at the higher discharges.

Acknowledgements

The author acknowledges Prof. Dr. Jorge Matos (IST, Portugal) for his support and guidance, along with Dr. Teresa Viseu (LNEC, Portugal) and Dr. Stefan Felder (UNSW, Australia) for granting access to the experimental facility and equipment, respectively.

References

[1] Khanh, M. H. T. (2017). History and development of Piano Key Weirs in Vietnam from 2004 to 2016. In Labyrinth and Piano Key Weirs III: Proceedings of the 3rd International Workshop on Labyrinth and Piano Key Weirs (PKW 2017), February 22-24, 2017, Qui Nhon, Vietnam (p. 3). CRC Press.

[2] Erpicum, S., Archambeau, P., Dewals, B. J., & Pirotton, M. (2017). Hydraulics of piano key weirs: a review. In Proceedings of the 3rd International Workshop on Labyrinth and Piano Key Weirs (pp. 27-36). CRC Press.

[3] Felder, S., & Pfister, M. (2017). Comparative analyses of phase-detective intrusive probes in high-velocity air–water flows. International Journal of Multiphase Flow, 90, 88-101.

[4] Reis, M. (2015). Estudo experimental do escoamento em descarregadores de cheias em degraus com soleira em teclado de piano. M.Sc. thesis, Instituto Superior Técnico, Lisbon (in Portuguese).

[5] Gomes, R. (2018). Emulsionamento de ar e dissipação de energia do escoamento em descarregadores de cheias em degraus com soleira em teclado de piano. M.Sc. thesis, Instituto Superior Técnico, Lisbon (in Portuguese).

[6] Lempérière, F., & Ouamane, A. (2003). The Piano Keys weir: a new cost-effective solution for spillways. International Journal on Hydropower & Dams, 10(5), 144-149.

[7] Laugier, F., Vermeulen, J., & Blancher, B. (2017). Overview of design and construction of 11 piano key weirs spillways developed in France by EDF from 2003 to 2016. In Labyrinth and Piano Key Weirs III: Proceedings of the 3rd International Workshop on Labyrinth and Piano Key Weirs (PKW 2017), February 22-24, 2017, Qui Nhon, Vietnam (p. 37). CRC Press.

[8] Machiels, O., Erpicum, S., Dewals, B. J., Archambeau, P., & Pirotton, M. (2010). Piano Key Weirs: the experimental study of an efficient solution for rehabilitation. WIT Transactions on Ecology and the Environment, 133, 95-106.

[9] Pralong, J., Vermeulen, J., Blancher, B., Laugier, F., Erpicum, S., Machiels, O., Pirotton, M., Boillat, J.L., Ribeiro, M.L., & Schleiss, A. J. (2011). A naming convention for the Piano Key Weirs geometrical parameters. Labyrinth and piano key weirs, 271-278.

[10] Matos, J., & Meireles, I. (2014). Hydraulics of stepped weirs and dam spillways: engineering challenges, labyrinths of research. In 11th National Conference on Hydraulics in Civil Engineering & 5th International Symposium on Hydraulic Structures: Hydraulic Structures and Society-Engineering Challenges and Extremes (p. 330). Engineers Australia.

[11] Ward, J. P. (2002). Hydraulic design of stepped spillways. Ph. D. thesis, Colorado State University, US.

[12] Gonzalez, C. A., & Chanson, H. (2004). Interactions between cavity flow and main stream skimming flows: an experimental study. Canadian Journal of Civil Engineering, 31(1), 33-44.

[13] Felder, S., & Chanson, H. (2015). Phase-detection probe measurements in high-velocity free-surface flows including a discussion of key sampling parameters. Experimental Thermal and Fluid Science, 61, 66-78.

[14] Felder, S. (2013). Air-water flow properties on stepped spillways for embankment dams: Aeration, energy dissipation and turbulence on uniform, non-uniform and pooled stepped chutes. Ph.D. thesis, The University of Queensland, Australia.

[15] Matos, J., Gomes, R. & Felder, S. (2019). Sensitivity analysis of the dual-tip phase detection probe. Personal notes.

[16] Lee, H. E., Lee, C., Kim, Y. J., Kim, J. S., & Kim, W. (2013). Power law exponents for vertical velocity distributions in natural rivers. Engineering, 5(12), 933.

[17] Matos, J. (2000). Hydraulic design of stepped spillways over RCC dams. In Intl Workshop on Hydraulics of Stepped Spillways (pp. 187-194). Balkema Publ.

[18] Matos, J. (1999). Emulsionamento de ar e dissipação de energia do escoamento em descarregadores em degraus. Ph. D. thesis, Instituto Superior Técnico De Lisboa, Portugal (in Portuguese).

[19] Meireles, I. (2004). Caracterizaçao do escoamento deslizante sobre turbilhoes e energia específica resiudal em descarregadores de Cheias em Degraus. M. Sc. thesis, Instituto Superior Técnico de Lisboa, Portugal (in Portuguese).